Glyndŵr University
Glyndŵr University Research Online

Chemistry   Materials Science

Trimethylplatinum(IV) complexes of anionic N/O and O/O donor ligands: synthesis, NMR and fluxional behaviour

Peter J. Heard
Glyndwr University, p.heard@glyndwr.ac.uk

Kenneth Kite

Abil E. Aliev

Follow this and additional works at: http://epubs.glyndwr.ac.uk/chem

Part of the Inorganic Chemistry Commons, Organic Chemistry Commons, and the Physical Chemistry Commons

Recommended Citation

Heard, P. J., Kite, K., and Alliev, A. E. (1998) "Trimethylplatinum(IV) complexes of anionic N/O and O/O donor ligands: synthesis, NMR and fluxional behaviour". Polyhedron, 17(15), 2543-2554

Trimethylplatinum(IV) Complexes of Anionic O/O and N/O Donor Ligands: Synthesis, NMR and Fluxional Behaviour.

Peter J. Heard,[a,*] Kenneth Kite[b] and Abil Aliev[c]

[a] *Department of Chemistry, Birkbeck College, Gordon House, 29 Gordon Square, London WC1, UK.*

[b] *Department of Chemistry, University of Exeter, Exeter, EX4 4QD, UK.*

[c] *Department of Chemistry, University College London, Christopher Ingold Laboratories, 20 Gordon Street, London WC1, UK.*

Abstract.

Reaction of pentan-2,4-dione, pyridine-2-carboxylic acid or pyridine-2,6-dicarboxylic acid with trimethylplatinum(IV) gives dimeric complexes of general formulae *fac*-[PtMe$_3$L]$_2$, in which the ionised ligand acts in a chelating and a bridging fashion. High-resolution solid-state ^{195}Pt NMR data shows that the two platinum atoms are equivalent; the chemical shielding anisotropy and the principal components of the shielding tensor are reported.   The complexes are soluble in co-ordinating solvents, yielding monomeric species of general formulae *fac*-[PtMe$_3$L(solvent)], which are fluxional.   The pyridyl adducts, *fac*-[PtMe$_3$L(py)] (L = pentan-2,4-dionate or pyridine-2-carboxylato), are also stereochemically non-rigid.   The energetics of the dynamic processes have been studied by standard ^{1}H band shape analysis techniques; $\Delta G^{\ddagger}$ (298 K) is in the range 69 - 86 kJ mol^{-1}.   Solid-state ^{13}C, and solution-state ^{13}C and ^{195}Pt NMR data are also reported.

Introduction.

The trimethylplatinum(IV) cation, $[PtMe_3]^+$, is highly versatile and forms a wide variety of complexes with both neutral and anionic donor ligands, many of which display dynamic structural behaviour.[1] Anionic donors ligands, such as β-diketonates, tend to form dimeric complexes of the type fac-$[PtMe_3L]_2$, in which the ionised ligand acts in both a bridging and chelating fashion.[2-5] We have reported previously the trimethylplatinum(IV) complexes of two monoximes, viz. butane-2,3-dione monoxime[6] (Hbdm) and 1-phenylpropane-1,2-dione 2-oxime[7] (Hppdm). In the former case, the ionised monoxime (bdm) behaves in an analogous fashion to the β-diketonate ligands, forming a dimeric complex, $[PtMe_3(bdm)]_2$. In contrast, ppdm acts as a simple chelating ligand, and a monomeric complex results; the sixth co-ordination site is occupied by a weakly bound water molecule. The monoximate complexes are only soluble in strongly co-ordinating solvents, such as dimethyl sulfoxide and methanol, forming solvated monomers of the type fac-$[PtMe_3L(solvent)]$, which are fluxional. The energetics of the dynamic stereochemical process were measured by two-dimensional exchange spectroscopy, and were found to be highly dependent on the solvent, but essentially independent of the monoxime.

It was therefore of interest to investigate other anionic N/O bidentate ligands to determine if they behave in a similar manner to the ionised monoximes, and to study the latent fluxional behaviour of the β-diketonate complexes. Accordingly, we report here on the trimethylplatinum(IV) complexes of pyridine-2-carboxylic acid, pyridine-2,6-dicarboxylic acid and pentan-2,4-dione.

Experimental.

Materials.

Pyridine-2-carboxylic acid (picolinic acid), pyridine-2,6-dicarboxylic acid (dipicolinic acid), pentan-2,4-dione (acetylacetone) and pyridine were purchased from Aldrich Chemical Company and used without further purification. Trimethylplatinum(IV) sulfate was prepared by our published procedure.[6]

Synthesis of complexes.

All manipulations were performed in the dark, to prevent the photo-reduction of the trimethylplatinum(IV) moiety. The complex $[PtMe_3(acac)(py)]$ (**4**) (acac = acetylacetonate, py = pyridine) was prepared by the published procedure.[8]

[(pentan-2,4-dionato)trimethylplatinum(IV)] (**1**).— Pentan-2,4-dione (0.2 cm^3, 195 mg, 1.95 mmol) and trimethylplatinum(IV) sulfate (100 mg, 0.16 mmol) were stirred in 20 cm^3 of water for *ca.* 0.5 h. Solid sodium acetate trihydrate (200 mg, 1.47 mmol) was then added, and a white precipitate of $[PtMe_3(acac)]_2$ formed immediately. The reaction mixture was stirred for *ca.* 1 h, then the solid was filtered off and purified by crystallisation from a 50:50 mixture of dichloromethane and pentane. Yield; 75 mg (69 %).

[(pyridine-2-carboxylato)trimethylplatinum(IV)] (**2**).— An aqueous solution of pyridine-2-carboxylic acid (273 mg, 2.22 mmol in 10 cm^3 of water) was added to a vigorously stirred aqueous solution of trimethylplatinum(IV) sulfate (720 mg, 1.12 mmol, in 20 cm^3 of water). A white precipitate formed immediately. Stirring was continued for *ca.* 1 h, then the solid was isolated by filtration. Recrystallisation from ethanol-water gave 730 mg (90 %) of (**2**).

[(pyridine-2-carbxylato-6-carboxylic acid)trimethylplatinum(IV)] (**3**).— Pyridine-2,6-dicarboxylic acid (100 mg, 0.60 mmol) was dissolved in 15 cm^3 of warm water (50 ^{o}C), and added to a stirred benzene solution of (**1**) (100 mg, 0.15 mmol in 15 cm^3). The reaction mixture was stirred at 50 ^{o}C for *ca.* 4 h, during which time a white solid formed at the phase boundary. The solid was isolated by filtration and recrystallised from ethanol-water. Yield; 50 mg (41 %).

[(pyridine)(pyridine-2-carboxylato)trimethylplatinum(IV) (**5**).— [(Pyridine-2-carboxylate)trimethylplatinum(IV)] (65 mg, 0.09 mmol) was dissolved in 2 cm^3 of dry pyridine, and the reaction mixture was warmed to *ca.* 60 ^{o}C for 1 h. The excess pyridine was then removed *in vacuo* and the crude residue purified by crystallisation from benzene-pentane. Yield; 64 mg (81 %).

Physical methods.

Fast atom bombardment (FAB) mass spectra were obtained at the London School of Pharmacy, on a VG Analytical ZAB-SE Instrument, using Xe^+ ion bombardment at 8 kV energy, on samples in a matrix of 3-nitrobenzyl alcohol.   Infrared spectra were recorded as pressed CsI discs on a Nicolet Magna 550 FT-IR spectrometer operating in the range 4000 - 220 cm^{-1}.   Elemental analyses were carried out at University College London.

Solution-state ^1H and ^{13}C NMR spectra were recorded in $(CD_3)_2SO$, $CDCl_3$ or $(CDCl_2)_2$ on a JEOL GSX270 Fourier transform spectrometer, operating at 270.06 MHz and 67.81 MHz, respectively.   Chemical shifts are quoted relative to tetramethylsilane an internal standard.   Solution-state ^{195}Pt NMR spectra were recorded in either $CHCl_3$ or CH_3OH (*ca*. 25 % v/v $CDCl_3$ was added for locking), on a Bruker AMX400 Fourier transform spectrometer, operating at 86.02 MHz.   Chemical shifts are quoted relative to the absolute frequency scale, $\Xi(^{195}Pt) = 21.4$ MHz.   The probe temperatures were controlled by standard variable temperature units, which were periodically calibrated; probe temperatures are considered accurate to within ± 1 ^oC.   The line shapes of the variable temperature ^1H NMR spectra were analysed using the dynamic NMR simulation programs[9,10] DNMR3 or DNMR5.   The 'best-fit' rate constants determined from the band shape fittings were used to calculate the Eyring activation parameters; errors quoted are those defined by Binsch and Kessler.[11]

High-resolution solid-state ^{13}C and ^{195}Pt NMR spectra were recorded at 75.5 MHz and 64.4 MHz, respectively, on a Bruker MSL300 Fourier transform spectrometer using a standard Bruker magic angle spinning probe, with a double-bearing rotation mechanism.   Spectra were recorded at ambient temperature (298 K) on polycrystalline powders in zirconica rotors with a 4 mm external diameter, and subjected to MAS at frequencies in the range 1.2 - 12 kHz.   Carbon-13 chemical shifts are quoted relative to tetramethylsilane, and ^{195}Pt chemical shifts are quoted relative to the absolute frequency scale, $\Xi(^{195}Pt) = 21.4$ MHz.   For ^{13}C spectra, the standard cross-polarisation (CP) technique was employed, with high power ^1H decoupling during acquisition.   Carbon-13 dipolar dephasing (NQS) spectra were

recorded using the Bruker program NQS.[12]   The optimum Hartmann-Hahn matching

condition for the ^{195}Pt CP spectra, was set using [PtMe$_3$Cl]$_4$, which proved more

sensitive than K$_2$Pt(OH)$_6$;[13] a reasonable signal was observed for

trimethylplatinum(IV) chloride after a single transient.   Typical experimental

parameters were: ^{13}C 90° pulse = 3.5 μs; ^{195}Pt 90° pulse = 3.7 μs; ^{1}H 90° pulse = 3.9

μs; CP contact time = 5 - 10 ms.

Results and discussion.

Pentan-2,4-dione (acetylacetone, acac-H), pyridine-2-carboxylic acid (picolinic acid,

pic-H) and pyridine-2,6-dicarboxylic acid (dipicolinic acid, dpaH$_2$) react with

trimethylplatinum(IV) synthons to form air-stable, crystalline complexes of general

formulae *fac*-[PtMe$_3$L]$_2$ (L = acac, pic or dpaH).   Analytical, IR and mass spectral

data indicate that they have the structures shown in Figure 1 (see below).

Complex (**1**) has been prepared previously from the reaction of trimethylplatinum(IV)

sulfate with sodium acetylacetonate[14] and from the reaction of trimethylplatinum(IV)

iodide with thallium acetylacetonate.[15]   However, we have found that it can be more

conveniently synthesised by the direct combination of pentan-2,4-dione and

trimethylplatinum(IV) sulfate (see above).   Reaction of complexes (**1**) and (**2**) with

pyridine (py) yields the 1:1 adducts, [PtMe$_3$(acac)(py)] (**4**) (which is known[8]) and

[PtMe$_3$(pic)(py)] (**5**); however, when [PtMe$_3$(dpaH)]$_2$ is treated with pyridine an

inseparable mixture of products is obtained.   The bipyridyl (bipy) adduct of (**1**),

[PtMe$_3$(bipy)(acac)], in which the acetylacetonate ligand is bound to the metal moiety

in a monodentate fashion via the γ-carbon atom, is also known,[8] but attempts to

prepare the bipy adducts of (**2**) and (**3**) were unsuccessful.

The structures of several trimethylplatinum(IV) β-diketone and related β-ketoester

complexes have been determined by neutron and X-ray diffraction techniques, and

have been to shown to be dimeric, with the ionised ligand acting in both a chelating

and bridging fashion.[2-5]   Although the crystal structure of (**1**) has not been

determined, ^{1}H NMR evidence[16] indicates that it is also dimeric.   The FAB mass

spectrum of (**1**) does not reveal the presence of any dimer, $[PtMe_3(acac)]_2$, in the gas-phase. However, a strong peak is observed at $m/z^+ = 340$, which corresponds to the monomeric unit, and analytical data are consistent with stoichiometry $[PtMe_3(acac)]$. The complex presumably dimerises in the solid-state, to achieve an octahedral 18-valence electron structure. The IR spectrum displays three bands in the C-H stretching region, characteristic of a *fac*-octahedral arrangement of the trimethylplatinum(IV) metal moiety.[17-19] Strong bands are also observed at 1610, 834, 650 and 600 cm^{-1}, characteristic of a terdentate bound diketone.[20,21] There are no bands indicative of a co-ordinated water molecule, which would be expected if the complex were monomeric.[7] Analytical data are reported in Table 1.

The micro analytical figures for complexes (**2**) and (**3**) show some deviation from those expected for the formulated species; the data tend to point towards monomeric aquo-complexes, *viz.* $[PtMe_3L(H_2O)]$ (L = pic or dpaH). However, there is no evidence of such species in the either the IR or FAB mass spectra of (**2**) or (**3**) The FAB mass spectrum of (**2**) displays strong peaks at $m/z^+ = 725$ and 363, which are due to $[PtMe_3(pic)]_2$ and $[PtMe_3(pic)]$, respectively. Complex (**3**) is rather more unstable, and totally fragments on ionisation; the strongest fragmentation peak occurred at $m/z^+ = 240$, which is due to the species $[PtMe_3]$, and no peaks due to $[PtMe_3(dpaH)]_2$ or $[PtMe_3(dpaH)]$ were observed. The IR spectra of (**2**) and (**3**) point towards dimeric species; no bands were observed which could be assigned to a co-ordinated water molecule. Analytical data for the pyridyl adducts, (**4**) and (**5**), (Table 1) are entirely consistent with the proposed structures.

Solid-state NMR studies.

Platinum-195 is a well-established NMR probe, which has been used extensively in solution-state studies.[22] However, the amount of solid-state ^{195}Pt NMR data in the literature is very limited. In a polycrystalline powder, the molecules are present in all possible orientations with respect to the external magnetic field, and as a result, the chemical shielding anisotropy (CSA, $\Delta\sigma$) and its principal components, σ_{11}, σ_{22} and σ_{33}, can be determined as well as the isotropic chemical shift, σ_{iso}. Magic angle spinning (MAS) of the sample at speeds in excess of the CSA effectively averages $\Delta\sigma$

to zero; only the isotropic band is then observed in the NMR spectrum.   However, the CSA of ^{195}Pt is generally very large ($\Delta\sigma \approx 1000$ ppm for Pt^{IV}) and it is not possible to attain sufficiently high MAS frequencies to average $\Delta\sigma$.   Thus in the MAS NMR spectrum, the isotropic peak is flanked on both sides by spinning side-bands, which are separated by multiple integers of the MAS frequency.   At very low MAS frequencies, the side-band envelope approximates the shape of the powder patter; consequently, the principal components of the CSA tensor can be determined.[23]   In terms of sensitivity, this approach has significant advantages over recording non-MAS powder patterns, and we have used this method to determine the principal components of the CSA tensor here.   Figure 2 shows the solid-state ^{195}Pt NMR spectra of (**1**) at three different MAS frequencies.

The data obtained for the complexes (**1**) - (**5**) are reported in Table 2.   The magnitudes of $\Delta\sigma$ and the asymmetry, η, obtained for the acetylacetonate complex, (**1**), are in good agreement with those obtained previously from the static powder pattern ($\Delta\sigma \approx 1123$ ppm, $\eta \approx 0.1$).[24]   Owing to the large isotropic chemical shift range of ^{195}Pt (*ca.* 10000 ppm), it is a very sensitive probe for the detection of chemical and crystallographic inequivalence.   The observation of a single isotropic signal for all five complexes thus indicates that the platinum sites are crystallographically equivalent in both the monomeric *and* dimeric complexes.   It is also noteworthy that the CSA tensor, $\left|\Delta\sigma\right|$, is significantly smaller for the monomeric pyridyl adducts, (**4**) and (**5**), than for the dimeric species (**1**) - (**3**).

Solid-state ^{13}C CP MAS NMR spectra were also acquired for all five complexes; data are reported in Table 3.   The spectra are closely analogous to those obtained in the solution-state (see below).   Spectral assignments were made by comparison with the solution-state spectra and on the basis non-quaternary suppression (NQS) experiments.   The multiple resonances observed for each chemical environment in the acetylacetonate complexes, (**1**) and (**4**), presumably result from crystallographic inequivalences.   The ^{13}C CP MAS NMR spectrum of (**1**) is shown in Figure 3.

Solution-state NMR studies.

The dimeric complexes (**1**), (**2**) and (**3**) are soluble in co-ordinating solvents, such as dimethyl sulfoxide, in which they form solvated monomers (see below).   The ambient temperature (298 K) ^{1}H NMR spectra of the complexes in $(CD_3)_2SO$ displayed well-resolved signals due to the species *fac*-[PtMe$_3$L(solvent)] [L = acac, pic or dpaH; solvent = $(CD_3)_2SO$].   On warming, the bands due to the platinum-methyl signals exhibit fully reversible dynamic NMR line broadening, due to an intramolecular exchange process.   The results obtained for the picoline carboxylate complex, (**2**), will serve to illustrate the analysis of the problem.   The spectrum of (**2**) at 298 K shows three platinum-methyl signals, with ^{195}Pt satellites, in a 1:1:1 intensity ratio, at $\delta = 0.97$, 0.93 and 0.71.   The three bands are readily assignable able to the Pt-Me groups *trans* O, *trans* N and *trans* S(solvent), respectively, on the basis of their $^2J_{PtH}$ scalar couplings (72.8, 69.0 and 69.7 Hz).[6,7]   The aromatic region of the spectrum shows four signals in a 1:1:1:1 intensity ratio.   The signal due to the picoline carboxylate α-hydrogen, H$_D$ (Fig. 1), is easily identified by its measurable coupling to ^{195}Pt ($^3J_{PtH} \approx 13$ Hz).   From H$_D$, an assignment of the signals due to the remaining picoline carboxylate-H atoms can be made on the basis of the scalar coupling network (COSY experiment).   Hydrogen-1 NMR data are reported in Table 3.

On warming, the bands due to the Pt-Me groups *trans* O and *trans* S(solvent) begin to broaden, whilst the signal due to the Pt-Me group *trans* N stays sharp.   These dynamic line shape changes indicate that the complex is undergoing an intramolecular 'windscreen-wiper' fluxional rearrangement (Figure 4), analogous to that observed previously for the monoxime complexes, [PtMe$_3$L(solvent)] (L = bdm or ppdm).[6,7] Above *ca*. 350 K, the *trans* N signals begins to broaden, presumably as a result of the well-established Pt-Me scrambling process.[25]   No changes were observed in the aromatic region of the spectra, and crucially, the magnitude of the ^3J(Pt-H$_\alpha$) scalar coupling is temperature independent.   This clearly establishes the 'windscreen-wiper' fluxion as an intramolecular process; the Pt-H$_\alpha$ coupling would be lost if the mechanism involved ligand dissociation.   The energetics of the 'windscreen-wiper' fluxion were measured by standard band shape analysis methods.   Nine accurate rate constants were measured in the temperature range 313 - 353 K, where the rate of

platinum-methyl scrambling was assumed to be negligible. The Eyring activation parameters are reported in Table 5.

The variable temperature NMR spectra of the acetylacetonate complex, (**1**), are exactly analogous to those of (**2**). However, in complex (**3**), a second fluxional process, which leads to an exchange of the Pt-Me groups *trans* O and *trans* N, occurs concomitant with the 'windscreen-wiper' rearrangement. This second fluxion presumably involves exchange of the pendant and co-ordinated carboxyl groups, in an analogous process to the 'tick-tock twist' rearrangement observed in bidentate complexes of terpyridine.[26] In solution, (**3**) gives rise to four degenerate species (Figure 5), which must all be considered in the analysis of the dynamic NMR problem. The two fluxional processes cause the inter-conversion of the three Pt-Me signals according to the dynamic spin system (**I**). The variable temperature NMR spectra were simulated on this basis. The complex is thermally unstable and the band shape fittings were complicated by the presence of peaks due to decomposition products; however, moderate fits were achieved, from which the Eyring activation parameters for the two *independent* dynamic processes were calculated (Table 5).

$$\begin{array}{ccc} ABC & \rightleftharpoons & ACB \\ \updownarrow & & \updownarrow \\ CBA & \rightleftharpoons & BCA \end{array}$$

(**I**)
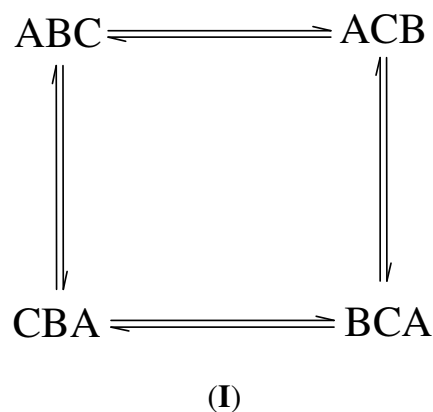
The ambient temperature (298 K) ^{1}H NMR spectra of the pyridyl adducts, (**4**) and (**5**), in CDCl$_3$ displayed well-resolved signals, characteristic of stereochemically rigid structures. The spectra are analogous to those of complexes (**1**) and (**2**), except for the presence of additional signals due to the co-ordinated pyridine ring. The pyridine-Hα environments, H$_E$/H$_{E'}$ (Fig. 1), are readily identified because of the measurable $^3J_{PtH}$

scalar couplings (*ca*. 11 Hz), and the *meta* and *para* environments can be distinguished by their relative intensities (2:1). Hydrogen-1 NMR data are reported in Table 4.

Warming the sample to *ca*. 330 K (the maximum limit for $CDCl_3$ solutions) does not lead to any dynamic band shape changes; however, at temperatures in excess of *ca*. 350 K [in $(CDCl_2)_2$ solution], the Pt-Me signals broaden, coalesce and eventually sharpen to give a single resonance, with ^{195}Pt satellites. Concomitant with these band shape changes is a loss of the $^3J_{PtH}$ scalar coupling to $H_E/H_{E'}$, indicating that the Pt-N(py) bond is labile at these temperatures. The ^3J(Pt-H_D) [Pt-Hα(pic)] scalar coupling is temperature independent. The band shape changes observed in the Pt-Me region presumably result from a combination of platinum-methyl scrambling[25] and the 'windscreen-wiper' fluxion,[6,7] initiated by the dissociation of the pyridine ligand. The energetics were measured by standard band shape analysis of the Pt-Me signals. Ten reliable fits were obtained for (**4**), six of which are shown in Figure 6. Activation parameters are reported in Table 5.

Carbon-13 NMR spectra were also acquired for all five complexes. Signals were assigned on the basis of their chemical shifts.[27] Data, which are fully consistent with the formulated species, are reported in Table 5.

Solution-state ^{195}Pt NMR spectra were obtained, for comparison with the solid-state spectra (see above). The ambient temperature (298 K) ^{195}Pt NMR spectra of complexes (**2**) - (**5**) each display a single, sharp band; the isotropic chemical shifts (Table 2) are within $\pm$ 40 ppm of those observed in the solid-state. The acetylacetonate complex, (**1**), displays two sharp signals, of different intensity, at δ = 2430 and 2768. The isotropic shift of the low frequency band is close to that observed in the solid-state. This is presumably due to the dimeric species, $[PtMe_3(acac)]_2$, which is thought to be retained in chloroform solution (although it has been shown that an *intermolecular* dimer-dimer exchange takes place, which probably involves a monomeric transition-state species).[16b] The ratio of the populations of the two species is 93:7 at ambient temperature; however, the high frequency band gradually increases in intensity on cooling, and at *ca*. 215 K, the ratio is 58:42. A signal due to a third,

minor species appears below *ca*. 240 K at $\delta \approx 2720$.   The natures of the two minor solution-state species are not known (see below).

It is noteworthy that the isotropic chemical shifts of complexes (**1**) - (**3**) in solution (where they exist as solvent co-ordinated monomers) are very similar to those observed for the dimers in the solid-state.   This clearly shows that the co-ordinated solvent molecule (methanol) has only a negligible effect on the chemical environments of the platinum atoms.

A low temperature (*ca*. 225 K) ^{1}H NMR spectrum for (**1**) was recorded in CDCl$_3$, in an attempt to identify the nature of the minor species observed in the [195]Pt NMR spectra (see above).   However, the data obtained were in full accord with that previously published,[16] and no evidence of any minor species was found.   Thus the origins of the additional signals observed in the [195]Pt spectra of (**1**) remain uncertain.

Activation energies.

The activation parameters obtained for the fluxional processes in the five complexes are reported in Table 5.   Examination of this data reveals a number of points.

(i) The magnitudes of the free energies of activation, $\Delta G^{\ddagger}$ (298 K), for the monoxime complexes, [PtMe$_3$L(solvent)] [L = butane-2,3-dionate monoxime (bdm) or 1-phenylpropane-1,2-dionate 2-monoxime (ppdm); solvent = dimethyl sulfoxide, methanol or acetone], reported previously were found to be highly dependent on the solvent, but essentially independent of the monoxime.[6,7]   This suggests that the largest contribution to $\Delta G^{\ddagger}$ comes from the energy required to break the Pt-solvent bond.   Complexes (**1**) and (**2**) have very similar activation energies; however, the absolute magnitudes are *ca*. 15 kJ mol^{-1} lower than for the monoximates, in the same solvent (dimethyl sulfoxide); this points to much weaker Pt-S(solvent) bonds in (**1**) and (**2**).   By way of contrast, complex (**3**) has a similar magnitude for $\Delta G^{\ddagger}$ (298 K) to the bdm and ppdm complexes.   These trends are difficult to rationalise. The different interactions between the metal centre and the anionic ligands will

clearly have some effect on the relative strengths of the Pt-solvent bonds (although *cis* interactions are generally small). However, since the net effects of the Pt-(monoximate), Pt-(acac), Pt-(pic) and Pt-(dpaH) interactions are all likely to be significantly different from each other, this does not readily rationalise the observed trends. It seems unlikely that steric factors play a large rôle (although where present, such effects can be significant[28-30]), since both the monoximes and the ligands studied here are essentially planar. Thus the factors that influence the energetics are obviously complex, and it appears probable that the similarity in the free energies of activation for (**1**) and (**2**) are coincidental.

(ii) The activation energies for the fluxional processes in (**4**) and (**5**) are similar; this might be expected, since the free energies of activation in (**1**) and (**2**) are also similar (see above). The largest contribution to $\Delta G^{\ddagger}$ is likely to be the energy required to break the Pt-N(pyridine) bond (see above), thus the higher magnitudes of $\Delta G^{\ddagger}$ (298 K) for (**4**) and (**5**), compared to (**1**) and (**2**), presumably reflects the relative strengths of the Pt-N(pyridine) and Pt-S(dimethyl sulfoxide) bonds in these complexes.

(iii) The free energy of activation for the carboxyl group exchange (the 'tick-tock twist' rearrangement) in (**3**) [$\Delta G^{\ddagger}$ (298 K) = 69.4 kJ mol^{-1}] is notably higher than for analogous processes in neutral trimethylplatinum(IV) halide complexes, such as [PtXMe$_3$(2,2':6,2''-terpyridine)][26] and [PtXMe$_3$\{2,6-bis(p-tolylthiomethyl)pyrdine\}][31] (X = halogen). This is presumably because increased electrostatic interactions between the charged [PtMe$_3$]$^+$ moiety and the anionic ligand lead to stronger metal-ligand bonds. Similar trends have been observed recently in trimethylplatinum(IV)-pyridazine complexes.[28,29]

The mechanisms of the 'windscreen-wiper' and 'tick-tock twist' fluxions have been discussed in some detail previously.[6,7,26]

References.

1. R. B. King (Ed), *Encyclopaedia of Inorganic Chemistry*, Wiley, New York, 1994, Volume 5 p 2581 *et seq*.

2. A. C. Hazell and M. R. Truter, *Chem. Ind.(London)*, 1959, 564.

3. A. C. Hazell and M. R. Truter, *Proc. Roy. Soc. A*, 1960, **252**, 218.

4. A. G. Swallow and M. R. Truter, *Proc. Roy. Soc. A*, 1960, **252**, 205.

5. R. N. Hargreaves and M. R. Truter, *J. Chem. Soc. A*, 1969, 2282.

6. E. W. Abel, P. J. Heard, K. Kite, K. G. Orrell and A. F. Psaila, *J. Chem. Soc., Dalton Trans*., 1995, 1233.

7. P. J. Heard and K. Kite, *J. Chem. Soc., Dalton Trans*., 1996, 3543.

8. K. Kite and M. R. Truter, *J. Chem. Soc. A*, 1968, 934.

9. D. A. Kleier and G. Binsch, DNMR3, *Quantum Chemistry Program Exchange*, Indian University.

10. D. S. Stephenson and G. Binsch, DNMR5, *Quantum Chemistry Program Exchange*, Indian University.

11. G. Binsch and H. Kessler, *Angew. Chem., Int. Ed. Engl*., 1980, **19**, 411.

12. S. J. Opella and M. H. Fry, *J. Am. Chem. Soc*., 1979, **101**, 5855.

13. R. K. Harris, P. Reams and K. J. Packer, *J. Chem. Soc., Dalton Trans*., 1986, 1015.

14. J. R. Hall and G. A. Swile, *J. Organomet. Chem*., 1973, **47**, 195.

15. R. C. Menzies, *J. Chem. Soc*., 1928, **130**, 565.

16. (a) J. R. Hall and G. A. Swile, *J. Organomet. Chem*., 1970, **21**, 237; (b) N. S. Ham, J. R. Hall and G. A. Swile, *Aust. J. Chem*., 1975, **28**, 759..

17. D. E. Clegg, J. R. Hall and G. A. Swile, *J. Organomet. Chem*., 1972, **38**, 402.

18. A. J. Downs, D. A. Long and L. A. K. Stavely (Eds), *Essays in Structural Chemistry*, Macmillan, London, 1974, p 433.

19. A. F. Psaila, *Ph.D. Thesis*, University of Exeter, 1977.

20. K. Kite, *Ph.D Thesis*, University of Leeds, 1965.

21. R. D. Gillard, H. G. Silver and J. L. Wood, *Spectrochem. Acta*, 1964, **20**, 63.

22. P. S. Pregosin (Ed), *Transition Metal NMR*, Elsevier, Amsterdam, 1991.

23. J. Herzfeld and A. E. Berger, *J. Chem. Phys*., 1980, **73**, 604.

24. D. M. Doddrell, P. F. Barron, D. E. Clegg and C. Bowie, *J. Chem. Soc., Chem. Commun*., 1982, 575.

25. E. W. Abel, S. K. Bhargava and K. G. Orrell, *Prog. Inorg. Chem*., 1984, **32**, 1.

26. E. W. Abel, V. S. Dimitrov, N. J. Long, K. G. Orrell, A. G. Osborne, V. Sik, H. B. Hursthouse and M. A. Mazid, *J. Chem. Soc., Dalton Trans*., 1993, 291.

27. J. B. Stothers, *Carbon-13 NMR Spectroscopy*, Academic Press, London, 1972.

28. P. J. Heard, *Ph.D. Thesis*, University of Exeter, 1994.

29. E. W. Abel, P. J. Heard, K. G. Orrell, M. B. Hursthouse and K. M. A. Malik, *J. Chem. Soc., Dalton Trans*., 1995, 3165.

30. E. W. Abel, P. J. Heard and K. G. Orrell, *Inorg. Chim. Acta*, 1997, **255**, 65.

31. E. W. Abel, P. J. Heard, K. G. Orrell, M. B. Hursthouse and M. A. Mazid, *J. Chem. Soc., Dalton Trans*., 1993, 3795.

32. U. Haeberlen, *Adv. Magn. Reson. (Suppl. 1)*, Academic Press, 1976.

Table 1. Analytical data for complexes (**1**) - (**5**).

Complex	m/z[a]	Infrared[b]		Analysis[c]		
		v(PtC-H)	v(ligand)	C	H	N
(**1**)	340, 240	2956 2900 2817	1610, 1454, 1411, 1359, 834, 650, 600	28.32 (28.34)	4.37 (4.75)	
(**2**)	725, 602, 363, 333, 240	2956 2897 2816	1630, 1594, 1570,	28.55 (29.84)	3.81 (3.59)	3.47 (3.87)
(**3**)	240	2986 2903	1633, 1605	28.53 (29.56)	3.35 (3.22)	3.05 (3.45)
(**4**)	419, 389, 373, 319, 302, 289, 274, 240	2956 2894 2817	1603, 1579, 1550, 1524, 1448, 1394, 1350, 1069, 1044, 765, 702	37.45 (37.32)	4.79 (5.06)	3.24 (3.35)
(**5**)	442, 396, 363, 333, 274, 240	2953 2893 2817	1661, 1639, 1606, 1572, 1063, 766, 704	38.12 (38.10)	3.99 (4.11)	6.12 (6.35)

[a] Mass spectral data (major diagnostic bands).

[b] Recorded as pressed CsI discs (major diagnostic bands).

[c] Calculated values in parentheses.

Table 2.   Platinum-195 NMR data[a] for complexes (**1**) - (**5**).

Complex	δ(solution)[b]	δ_{iso}	δ_{11}	δ_{22}	δ_{33}	$\Delta\sigma$	η
(**1**)	2430 (93)[c] 2768 (7)[c]	2457	2912	2755	1702	1132	0.21
(**2**)	2438	2427	1691	2398	3192	-1147	0.92
(**3**)	2470	2450	3211	2493	1648	1204	0.90
(**4**)	2611	2644	2923	2718	2291	530	0.58
(**5**)	2260	2304	2742	2376	1794	765	0.72

[a] Data recorded at 298 K; chemical shifts quoted relative to the absolute frequency scale Ξ(^{195}Pt = 21.4 MHz); CSA tensors assigned according to Haeberlen's convention,[32] $\delta_{ij} = -\sigma_{ij}$, $\delta_{iso} = (\delta_{11}+\delta_{22}+\delta_{33})/3$, $\Delta\sigma = [(\delta_{11}+\delta_{22})/2]-\delta_{33}$, $\eta = (\delta_{11}-\delta_{22})/(\delta_{iso}-\delta_{33})$.

[b] Complexes (**1**), (**2**) and (**3**) recorded in $CH_3OH/CDCl_3$ (3:1 v/v) solution; complexes (**4**) and (**5**) recorded in $CHCl_3/CDCl_3$ (3:1 v/v) solution.

[c] Populations (%) given in parentheses, see text.

Table 3. Solid-state ^{13}C NMR data[a] for complexes (**1**) - (**5**).

Complex	δ(Pt-CH$_3$)[b]	δ(C$_1$)	δ(C$_2$)	δ(C$_3$)	δ(C$_4$)	δ(C$_5$)	δ(C$_6$)	(C$_7$)δ	δ(C$_{pyridyl}$)
(**1**)	-12.37(759) (1) -11.65(757) (2) -10.64(740) (1) -4.92(714) (2)	196.96 197.42 197.82	31.26 31.87 32.48 33.09	79.07(70)[c] 79.44(60)[c]					
(**2**)	-11.57(790) (1) -8.53(732) (2)	174.04	149.85	129.73	129.73	140.24	144.53		
(**3**)	-9.72(760) (1) -8.45(740) (1) -7.65(720) (1)	171.62	152.40	131.22	128.87	142.87	147.66	166.45	
(**4**)	-13.05(746) (1) -10.62(766) (2)	185.74 186.62	28.15 30.35	101.73					148.41, 151.74 (C$_{ortho}$); 128.58, 127.73 (C$_{meta}$); 139.02 (C$_{para}$)
(**5**)	-9.80(736) (1) -7.48(700) (1) -5.16(666) (1)	171.59	151.69	128.07	128.07	139.03	144.18		128-150[d]

[a] Data recorded at ambient temperature; chemical shifts quoted relative to tertramethylsilane; see Fig. 1 for labelling.

[b] $^2J_{PtC}$/Hz and number of methyl groups giving rise to the resonance are given in parentheses.

[c] $^3J_{PtC}$ given in parentheses.

[d] Broad unresolved signals.

Table 4. Hydrogen-1 NMR data[a] for complexes (**1**) - (**5**).

Complex	$\delta(\text{Pt-C}\mathbf{H}_3)^b$	$\delta(H_A)^c$	$\delta(H_B)^c$	$\delta(H_C)^c$	$\delta(H_D)^c$	$\delta(H_E/H_{E'})^c$	$\delta(H_F/H_{F'})^c$	$\delta(H_G)^c$
(**1**)	0.78(69.9) (1) (S) 0.86(73.6) (2) (O)	1.86	5.28(~3[d])					
(**2**)	0.71(69.7) (1) (S) 0.93(69.0) (1) (N) 0.97(72.8) (1) (O)	8.12(7.8, 1.4)	8.25(7.8, 7.7, 1.5)	7.88(7.7, 5.6, 1.4)	8.68(5.6, 1.5; 14.2[e])			
(**3**)	0.52(67.0) (1) (S) 0.86(74.5) (1) (O) 1.11(72.2) (1) (N)	8.24(7.7)	8.31(7.7, 7.7)	8.00(7.7)				
(**4**)	0.85(71.1) (1) (N-py) 1.00(73.6) (2) (O)	1.90	5.13(~3[d])			8.52(6.4, 1.5; 10.8[e])	7.41(6.4, 7.6)	7.83 (7.6, 1.5)
(**5**)	0.82(71.0) (1) (N-py) 1.13(73.6) (1) (O) 1.17(69.4) (1) (N)	8.23(7.8, 1.3)	7.97(7.8, 7.6, 1.5)	7.64(7.6, 5.5, 1.3)	8.63(5.5, 1.5; 11.9[e])	8.52(6.4, 1.3; 10.8[e])	7.33(6.4, 7.6)	7.76(7.6, 1.3)

[a] Spectra recorded at ambient temperature in $(CD_3)_2SO$ or $CDCl_3$ solution (see text); chemical shifts quoted relative to tetrametylsilane; see Fig. 1 for labelling.

[b] $^2J_{PtH}$/Hz, number of methyls giving rise to the resonance and the *trans* atom are given in parentheses.

[c] $^nJ_{HH}$/Hz given in parentheses.

[d] $^4J_{PtH}$/Hz.

[e] $^3J_{PtH}$/Hz.

Table 5.   Eyring activation parameters[a] for complexes (**1**) - (**5**).

Complex	$\Delta H^{\ddagger}$/kJ mol^{-1}	$\Delta S^{\ddagger}$/J mol^{-1} K^{-1}	$\Delta G^{\ddagger}$/kJ mol^{-1}
(**1**)	113.3 (1.9)	[b]	73.68 (0.16)
(**2**)	89.6 (1.7)	56 (5)	72.85 (0.18)
(**3**)	173 (19)	[b]	86 (2)
	61.7 (5.2)[c]	-26 (16)[c]	69.39 (0.44)[c]
(**4**)	93.8 (2.4)	42 (6.)	81.17 (0.45)
(**5**)			82[d]
			86[e]

[a] Data refers to the windscreen-wiper process except [c, d] and [e]; errors given in parentheses; $\Delta G^{\ddagger}$ quoted at 298 K except [d] and [e].

[b] Data unreliable due to narrow temperature range.

[c] Data for carboxyl group exchange.

[d] Data for combined windscreen-wiper/Pt-Me scrambling (see text); $\Delta G^{\ddagger}$ calculated from band coalescence, T_c = 403 K.

[e] Data for combined windscreen-wiper/Pt-Me scrambling (see text); $\Delta G^{\ddagger}$ calculated from initial band broadening, T_i = 353 K.

Table 6.   Solution-state ^{13}C NMR data for complexes (**1**) - (**5**).

Complex	$\delta(Pt\text{-}CH_3)^b$	$\delta(C_1)$	$\delta(C_2)$	$\delta(C_3)$	$\delta(C_4)$	$\delta(C_5)$	$\delta(C_6)$	$(C_7)\delta$	$\delta(C_{pyridyl})$
(**1**)	-12.98(725.5) (2) ^{c} (1)	186.21(12.8)	28.10(9.2)	100.45(31.3)					
(**2**)	-11.91 (669.8) (1) -10.04(664.9) (1) 2.34^d (1)	170.94	151.22	128.73	128.05	140.32	145.24		
(**3**)	-11.10^d (1) -6.66(673) (1) 2.41^d (1)	170.68	152.63	129.17	127.58	141.44	151.53	166.37	
(**4**)	-12.26(763.5) (2) -9.61(722.2) (1)	186.18(13.4)	28.90	100.16(29.7)					125.55(10.9) 137.88 149.02
(**5**)	-11.17(751.9) (1) -8.55(691.3) (1) -7.91(688.5) (1)	172.34	152.63	128.87(12.5)	127.91	139.17(12.5)	143.56(14.6)		125.95(9.8) 138.21 148.92

^{a} Data recorded at ambient temperature; chemical shifts quoted relative to tertramethylsilane; see Fig. 1 for labelling; $^nJ_{PtC}$/Hz given in parentheses; complexes (**1**) - (**3**) recorded in $(CD_3)_2SO$ solution; complexes (**4**) - (**5**) recorded in $CDCl_3$ solution.

^{b} $^1J_{PtC}$/Hz and number of methyl groups giving rise to the resonance are given in parentheses.

^{c} Band not observed.

^{d} Platinum-195 satellites not observed.

Figure Legends

Figure 1.   The structures of complexes (**1**) - (**5**), showing the hydrogen atom (A - G) and carbon atom (1 - 7) labelling schemes.

Figure 2.   Solid-state 64.4 MHz ^{195}Pt CP MAS spectra of (**1**) at three different MAS frequencies.   The isotropic peak is denoted *.   The MAS frequencies are shown along side.

Figure 3.   Solid-state 75.5 MHz ^{13}C CP MAS spectrum of (**1**), showing the Pt-Me and acac-Me regions.

Figure 4.   The proposed mechanism for the 'windscreen-wiper' fluxion, showing the effect of the rearrangement on the Pt-Me environments.   Methyl groups are numbered 1 - 3, and the letters identify the chemical environments.

Figure 5.   The four degenerate solution-state species of complex (**3**), and the inter-conversion pathways between them.   The 'windscreen-wiper' fluxion leads to pathways k_2 and k_4, and the 'tick-tock twist' fluxion leads to pathways k_1 and k_3; note that $k_1 = k_3$ and $k_2 = k_4$, giving two independent rate processes. The 'tick-tock twist' fluxion presumably also involves a rapid hydrogen ion transfer.

Figure 6.   Experimental and computer simulated variable temperature ^{1}H NMR spectra of complex (**4**).   'Best-fit' rate constants, k, for the combined windscreen-wiper/Pt-Me scrambling process are shown along side.